

Cite this: *Chem. Sci.*, 2020, **11**, 7188

All publication charges for this article have been paid for by the Royal Society of Chemistry

Received 9th April 2020
Accepted 20th June 2020

DOI: 10.1039/d0sc02065f
rsc.li/chemical-science

Introduction

Oxalamide skeletons are prevalent in many biologically active molecules and pharmaceuticals, such as Lixiana (**1**, Fig. 1), widely used as an anticoagulant.¹ Oxalamide **2** shows promising antiviral activity of entry inhibitors targeting the CD₄-binding site of HIV-1.² Additionally, oxalamides are employed as robust ligands in copper catalyzed cross coupling reactions (*e.g.*, oxalamides **3–5**).³ Besides these, oxalamides are also popular in food processing as flavoring agents (oxalamide **6**)⁴ and in drug delivery as a synthon of organosilica nanoparticles (oxalamide **7**).⁵ Given the importance of oxalamides, there is considerable interest in the development of novel, efficient protocols for their preparation.

Conventional methods for the synthesis of oxalamides are largely based on the reaction of oxalic acid with thionyl chloride to form oxalyl chloride followed by treatment with amines (Fig. 2a).^{3,6} Other methods such as oxidative carbonylation of amines using carbon monoxide^{7a,b} and aminolysis of oxalates^{7c,d} also lead to the formation of oxalamides. However, these methods are either not atom economic, generate stoichiometric amounts of waste, or involve acrid or toxic agents. Therefore, the development of atom-economic green and sustainable methods for the efficient construction of oxalamides is highly

desirable and remains an important goal both in chemical and pharmaceutical industries.

In 2007, we reported the ruthenium catalyzed dehydrogenative coupling of alcohols with amines leading to the environmentally benign synthesis of amides with H₂ liberation as the sole byproduct (Fig. 2b).⁸ Guan's group^{9a} and our group^{9b} also demonstrated the ruthenium pincer complex catalyzed dehydrogenative coupling of diols and diamines, to form polyamides. Other Ru-catalyzed systems for the synthesis of amides from amines and alcohols were subsequently reported.¹⁰ Recently, we,^{11a–d} Prakash^{11e} and Liu groups^{11f} have developed several liquid organic hydrogen carrier systems based on amide bond formation and the reverse hydrogenation reactions.

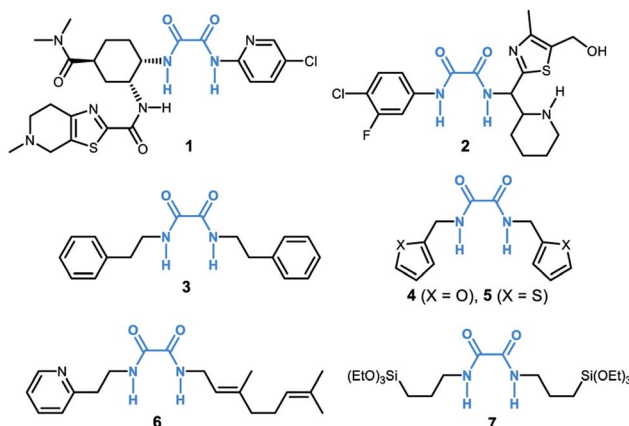


Fig. 1 Representative examples of functional molecules containing an oxalamide moiety.

^aDepartment of Organic Chemistry, Weizmann Institute of Science, Rehovot 76100, Israel. E-mail: david.milstein@weizmann.ac.il

^bChemical Research Support, Weizmann Institute of Science, Rehovot 76100, Israel

[†] Electronic supplementary information (ESI) available. CCDC 1957818. For ESI and crystallographic data in CIF or other electronic format see DOI: 10.1039/d0sc02065f

[‡] You-Quan Zou and Quan-Quan Zhou contributed equally.

[§] Present address: Department of Chemistry, University of Cambridge, Lensfield Road, Cambridge CB2 1EW, UK.



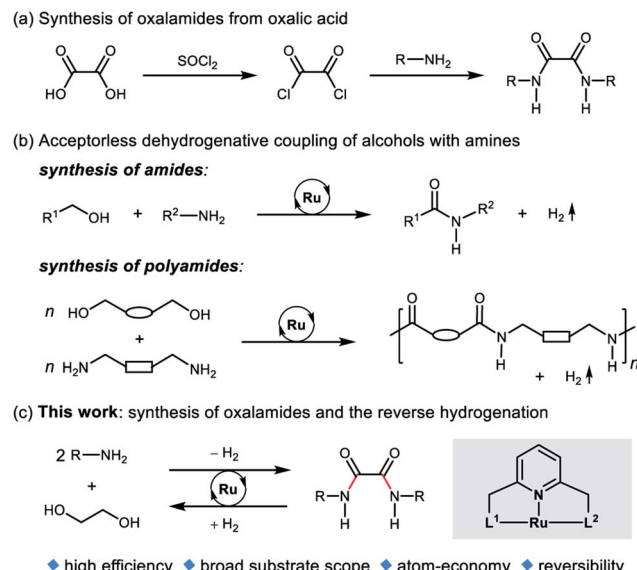


Fig. 2 (a) Conventional synthesis of oxalamides, (b) dehydrogenative amide bond formation, and (c) this work.

Ethylene glycol (EG) is an inexpensive and convenient feedstock in industry,¹² which can be accessed from renewable biomass-derived hydrocarbons.¹³ Very recently, we disclosed a reversible liquid organic hydrogen carrier system based on EG, capable of chemically loading and unloading hydrogen.¹⁴ In this system, EG undergoes acceptorless dehydrogenative esterification to oligoesters, and then the oligoesters are hydrogenated back to EG by using a ruthenium pincer catalyst. As part of our ongoing research program on green and sustainable homogeneous catalysis, we herein report an atom-economic and environmentally benign strategy for the direct synthesis of oxalamides *via* acceptorless dehydrogenative coupling of EG with amines (Fig. 2c). A potential challenge is the coordination ability of oxalamides as chelating ligands,³ which could possibly result in product inhibition.

We envisioned that dehydrogenative coupling of EG and the amine will first form an α -hydroxy amide. Subsequently, the resulting α -hydroxy amide would react with another molecule of amine to form the desired oxalamide *via* a similar catalytic cycle. In addition, the reverse hydrogenation of oxalamides back to EG and amines was also investigated using the same catalyst. To the best of our knowledge, there has hitherto been no report on acceptorless dehydrogenative synthesis of oxalamides from EG and amines, the only byproduct being hydrogen gas, valuable by itself.

Results and discussion

To examine the feasibility of the acceptorless dehydrogenative coupling of ethylene glycol and amines, our initial studies were focused on the reaction of EG and hexan-1-amine (**8a**). At the beginning, we tested the catalytic efficiency of ruthenium pincer complex **Ru-1**¹⁵ which upon deprotonation forms the dearomatized complex and catalyzes the synthesis of amides and

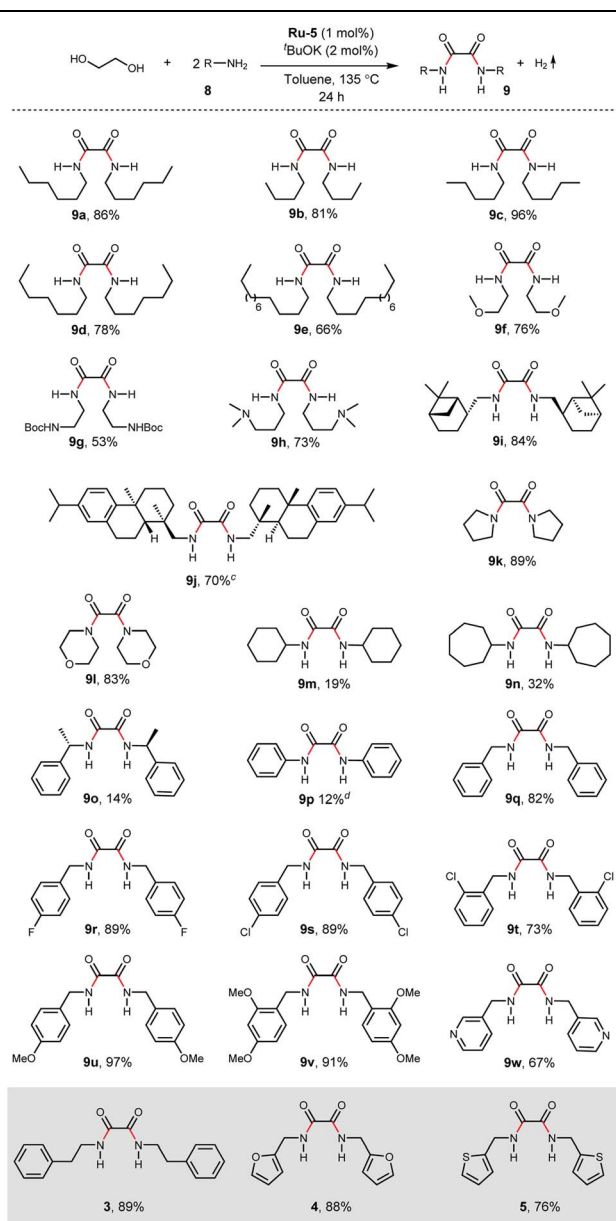
polyamides from amines and alcohols.⁸ The reaction did indeed take place using **Ru-1** (1 mol%) and $^t\text{BuOK}$ (1 mol%) at 135 °C in a mixture of toluene and dimethoxyethane (v/v = 1/1) in a closed system, affording the desired oxalamide **9a** in 26% isolated yield after 24 hours (Table 1, entry 1). Using the bipyridine-derived catalysts **Ru-2**¹⁶ and **Ru-3**,¹⁶ the isolated yield of **9a** was improved to 50% (entries 2 and 3). Employing the PNNH-based complexes **Ru-4**¹⁷ and **Ru-5**¹⁷ resulted in the case of **Ru-5** a considerable yield of **9a** to 77% using 2 mol% of $^t\text{BuOK}$ (entry 5). Encouraged by this promising result, we next evaluated the solvent effect (entries 6–9). Using toluene as a sole solvent with **Ru-5** as the catalyst **9a** was isolated in 86% yield (entry 6). The dearomatized acridine-based complex **Ru-6**, previously used in the esterification of EG,¹⁴ only afforded product **9a** in 27% yield (entry 10). Accordingly, the optimal reaction conditions for the acceptorless dehydrogenative coupling are as depicted in entry 6: 1 mol% of **Ru-5** as catalyst, 2 mol% of $^t\text{BuOK}$ as base, 135 °C in 2.0 mL of toluene.

With the optimized reaction conditions in hand, we next examined the generality of this catalytic dehydrogenative coupling system using various amines. As shown in Table 2, various aliphatic amines such as hexan-1-amine (**8a**), butan-1-

Table 1 Optimization of the reaction conditions

Entry ^a	Ru	$^t\text{BuOK}$	Solvent	Yield ^b (%)
1	Ru-1	1 mol%	Toluene/DME	26
2	Ru-2	1 mol%	Toluene/DME	50
3	Ru-3	1 mol%	Toluene/DME	40
4	Ru-4	2 mol%	Toluene/DME	37
5	Ru-5	2 mol%	Toluene/DME	77
6	Ru-5	2 mol%	Toluene	86
7	Ru-5	2 mol%	DME	71
8	Ru-5	2 mol%	THF	84
9	Ru-5	2 mol%	1,4-Dioxane	81
10	Ru-6	—	Toluene	27

^a Reaction conditions: ethylene glycol (1.0 mmol), **8a** (3.0 mmol), **Ru** catalyst (1 mol%), $^t\text{BuOK}$ (1–2 mol%), and solvent (2.0 mL) at 135 °C (bath temperature) for 24 hours in a closed system. ^b Isolated yield. DME: dimethoxyethane; THF: tetrahydrofuran; Bn: benzyl. Bold row is indicative of optimal conditions.

Table 2 Substrate scope^{a,b}

^a Reaction conditions: ethylene glycol (1.0 mmol), **8** (3.0 mmol), **Ru-5** (1 mol%), ⁷BuOK (2 mol%), and toluene (2.0 mL) at 135 °C (bath temperature) for 24 hours. ^b Isolated yield. ^c A mixture of toluene (1.0 mL) and dioxane (1.0 mL) was used as the solvent. ^d 50 mol% of ⁷BuOK was used.

amine (**8b**), pentan-1-amine (**8c**), heptan-1-amine (**8d**), dodecan-1-amine (**8e**) as well as 2-methoxyethan-1-amine (**8f**) smoothly dehydrogenatively coupled with ethylene glycol to give the corresponding oxalamides **9a**–**9f** in good to excellent isolated yields (66–96%). *tert*-Butyl(2-aminoethyl)carbamate (**8g**) and *N*¹,*N*¹-dimethylpropane-1,3-diamine (**8h**) reacted with ethylene glycol forming the desired products in 53% (**9g**) and 73% (**9h**) yields. It is worth noting that (*-*)-*cis*-myrtanylamine (**8i**) and (+)-dehydroabietylamine (**8j**) could also be applied in this reaction

generating oxalamides **9i** and **9j** in 84% and 70% yields, respectively. The oxalamidation procedure was compatible with secondary amines as well, as shown in the reactions of pyrrolidine and morpholine to form oxalamides **9k** (89% yield) and **9l** (83% yield). As a limitation of the system, α -branched primary amines such as cyclohexanamine (**8m**), cycloheptanamine (**8n**) and (*S*)-1-phenylethan-1-amine (**8o**) produced the desired oxalamide products with lower yields (14–32%). The less nucleophilic aniline exhibited low reactivity and only delivered *N*¹,*N*²-diphenyloxalamide (**9p**) in 12% yield using 50 mol% of base. Benzylamines (**8q**–**8v**) reacted well, and various electron-withdrawing (**8r**–**8t**) and electron-donating groups (**8u**–**8v**) on the phenyl group did not interfere with the reaction efficiency, furnishing the desired products **9q**–**9v** in good yields (73–97% yields). It is worth mentioning that pyridine-containing amine **8w** also worked quite well and the desired product **9w** was isolated in 67% yield. Moreover, oxalamides 3–5 which were reported to act as ligands,³ were obtained in 76–89% yields. Compared to previously reported methods, this protocol is more atom-economic, sustainable and efficient.

Amines are an important class of compounds widely used in agrochemicals, pharmaceuticals and organic synthesis.¹⁸ Hydrogenation of amide bonds represents a green and straightforward method to access amines. Although efficient hydrogenation of amides to amines and alcohols catalyzed by pincer complexes was reported by several groups,¹⁹ there is only one example of catalytic hydrogenation of oxalamides (60 bar hydrogen gas, 160 °C).^{7b} Interestingly, the oxalamides synthesized by us *via* acceptorless dehydrogenative coupling of EG and amines could be fully hydrogenated back to the amines and ethylene glycol using the same catalyst **Ru-5**. As shown in Table 3, in the presence of 1 mol% of **Ru-5**, 4 mol% of ⁷BuOK and 40 bar of hydrogen gas at 135 °C in 2.0 mL of toluene, oxalamides **9a**–**9d** (entries 1–4), **9f**, **9i**, **9k** (entries 5–7), **9q**–**9v** (entries 8–13) and 3–5 (entries 14–16) were efficiently hydrogenated to form the corresponding amines and ethylene glycol in excellent yields within 24 hours (85–99% yields).

To get some insight into the reaction mechanism, complex **Ru-5** was treated with 1.1 equivalents of ⁷BuOK in 0.5 mL of THF at room temperature (Scheme 1a), resulting in immediate a color change of the transparent yellow solution to a homogeneous red brown solution, which exhibited a doublet at δ = 110.73 ppm ($^2J_{P-H}$ = 15 Hz) in the ³¹P{¹H} NMR spectrum in THF (Scheme 2b). Performing the reaction in d_8 -THF showed that the N–H proton disappeared and the two CH₂ groups of the P-arm and N-arm were still present, clearly indicating that the deprotonation took place at the N–H bond and complex **10** was formed (see ESI and Fig. S6–S9† for details). The hydride resonance of **10** appeared at δ = –18.13 ppm (doublet, $^2J_{P-H}$ = 40.0 Hz) in the ¹H NMR (see ESI, Fig. S6† for details). Using 2.2 equivalents of ⁷BuOK also produced complex **10** together with the formation of a new species at δ = 124.0 ppm (broad singlet) in the ³¹P{¹H} NMR, probably attributable to the doubly-deprotonated complex, as we observed before with the PNNH complex **Ru-4**.¹⁷

Upon treatment with 5.0 equivalents of ethylene glycol the above reaction mixture (either from 1.1 equivalents or 2.2

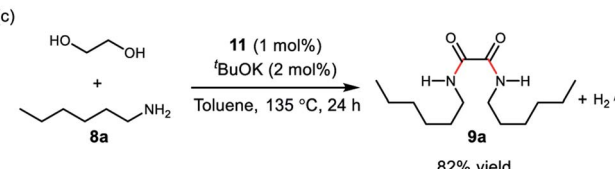
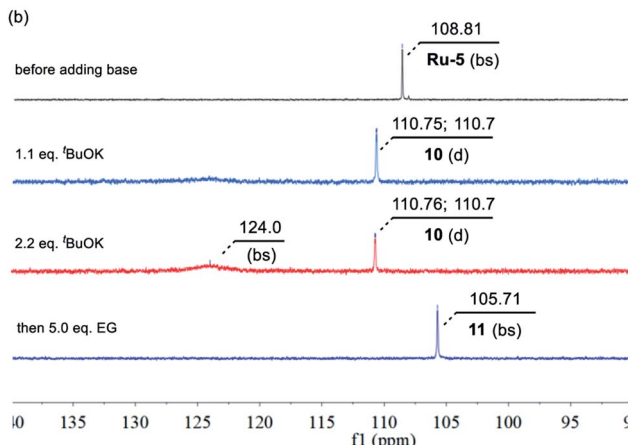
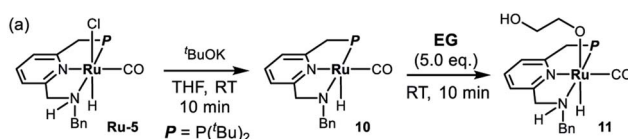
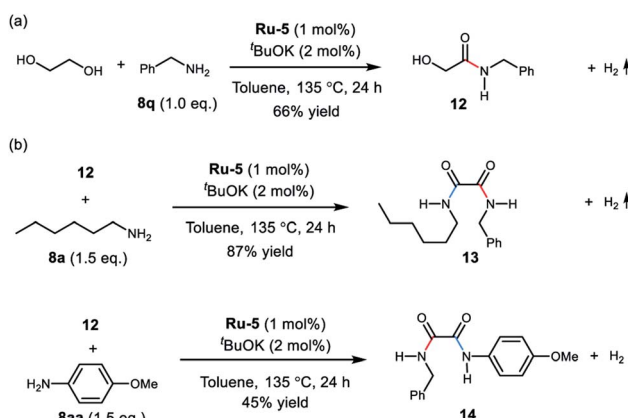


Table 3 Hydrogenation of oxalamides to ethylene glycol and amines

Entry ^a	9, 3–5	8	Yield ^b (%)		
				Ru-5 (1 mol%)	¹ BuOK (4 mol%)
1	9a	8a	95		
2	9b	8b	95		
3	9c	8c	97		
4	9d	8d	98		
5	9f	8f	86		
6	9i	8i	92		
7	9k	8k	85		
8	9q	8q	97		
9	9r	8r	99		
10	9s	8s	96		
11	9t	8t	99		
12	9u	8u	99		
13	9v	8v	99		
14	3	8x	95		
15	4	8y	98		
16	5	8z	95		

^a Reaction conditions: oxalamide (0.25 mmol), Ru-5 (1 mol%), ¹BuOK (4 mol%), H₂ (40 bar) and toluene (2.0 mL) at 135 °C (bath temperature) for 24 hours. ^b Yields were determined by ¹H NMR of the crude reaction mixture using mesitylene as an internal standard.

equivalents of base), a reddish brown solution was formed, generating complex 11, resulting from ethylene glycol addition to complex 10. Complex 11 exhibited a broad singlet at δ =

Scheme 1 (a) Deprotonation of Ru-5 and activation of ethylene glycol by complex 10, (b) the corresponding ³¹P{¹H} NMR spectra, and (c) the catalytic performance of complex 11.Scheme 2 (a) Synthesis of the α -hydroxy amide 12, and (b) the mixed oxalamides 13 and 14.

105.71 ppm in the ³¹P{¹H} NMR in THF (Scheme 1b) and in the ¹H NMR spectrum the hydride shifted downfield to δ = 16.03 ppm (doublet, J_{H-P} = 24.0 Hz), consistent with the alkoxide group of EG located *trans* to the hydride of complex 11 (see Fig. S10† for details). The IR spectrum of 11 showed a strong carbonyl absorption band at 1899 cm⁻¹ (Fig. S14†). Upon slow evaporation of a solution of 11 in a mixture of THF and pentane, crystals suitable for X-ray diffraction were formed. As shown in Fig. 3, a neutral distorted octahedral complex was generated with the

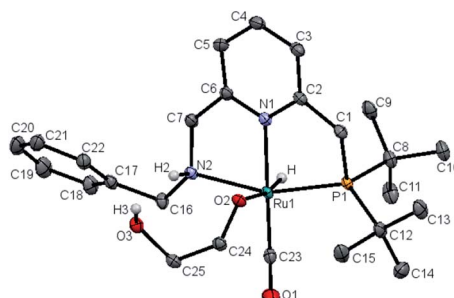
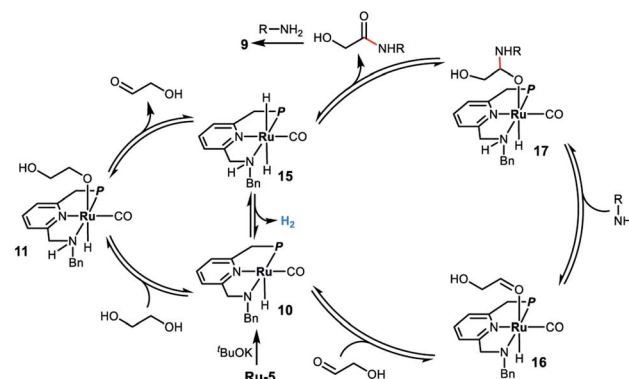


Fig. 3 X-ray crystal structure of complex **11**. Atoms are presented as thermal ellipsoids at 50% probability level. Hydrogen atoms are omitted for clarity except the hydride, H2 and H3. Selected bond lengths (Å) and angles (deg.): Ru(1)–C(23), 1.829(19); Ru(1)–N(1), 2.106(15); Ru(1)–N(2), 2.195(15); Ru(1)–O(2), 2.190(13); Ru(1)–P(1), 2.280(4); Ru(1)–H, 1.58(3); C(23)–Ru(1)–N(1), 178.10(7); N(2)–Ru(1)–P(1), 158.90(4); N(1)–Ru(1)–O(2), 80.98(5).

alkoxide group of EG coordinated to the ruthenium center. Upon heating complex **11** at 110 °C in d₈-toluene for 25 minutes, a new species which gave rise to signal at $\delta = 9.59$ ppm in the crude ¹H NMR, which might be attributed to the formation of glycolaldehyde (see ESI, Fig. S15† for details). Interestingly, using complex **11** as a catalyst, the desired product **9a** was isolated in 82% yield, indicating that **11** is a possible catalytic intermediate (Scheme 1c).

Interestingly, upon treatment EG with 1.0 equivalent of benzylamine under the optimal conditions, the mono-amidation product **12** was isolated in 66% yield (Scheme 2a). The α -hydroxy- amide **12** was also observed in the reaction of EG with two equivalents of benzylamine (see ESI, Fig. S16–S19 \dagger for details). These results support formation of the oxalamide product *via* an α -hydroxyamide intermediate. Moreover, reaction of amide **12** with hexan-1-amine (**8a**) afforded the mixed oxalamide **13** in 87% yield (Scheme 2b). The mixed aryl/alkyl oxalamide **14** was also successfully synthesised using *p*-anisidine as the arylamine coupling partner (45% yield). These results highlight the scope of this method for the synthesis of mixed oxalamides.

Based on the experimental results and previous work,^{8,11} we propose a possible reaction mechanism for the ruthenium homogeneously catalyzed acceptorless dehydrogenative coupling of ethylene glycol and amines to form oxalamides. As outlined in Scheme 3, deprotonation of **Ru-5** by ¹BuOK leads to complex **10**, which adds ethylene glycol to generate the alkoxide species **11** *via* metal ligand cooperation.²⁰ Although there is no vacant coordination site *cis* to the alkoxide ligand in complex **11**, hydride elimination can take place forming intermediate **15** *via* two alternative pathways. One involves the full dissociation of the alkoxide from **11**, followed by hydride abstraction from it by the ruthenium center;²¹ the other possibility is that proton and hydride directly transfer from ethylene glycol to deprotonated complex **10** without the formation of alkoxide **11**.²² The hydride elimination might also occur through the N-side arm dissociation. Subsequently, hydrogen evolution from complex **15** takes place, followed by coordination of the generated glycolaldehyde,²³ affording the saturated amido intermediate **16**.



Scheme 3 Proposed reaction mechanism for the ruthenium-catalyzed acceptorless dehydrogenative coupling of EG and amines to form oxalamides

Reaction of **16** with the amine forms the hemiacetal intermediate **17** followed by release of α -hydroxy amide to regenerate the *trans*-dihydride complex **15**. The formed α -hydroxy amide reacts with another molecule of amine to form the corresponding oxalamide **9** *via* a similar pathway. Finally, complex **15** releases a second molecule of hydrogen, regenerating complex **10** which then re-enters the catalytic cycle.

Conclusions

In conclusion, we have developed the acceptorless dehydrogenative coupling of ethylene glycol and amines with H_2 evolution, catalyzed by a ruthenium pincer complex, enabling the synthesis of oxalamides in an unprecedented highly atom-economic and sustainable manner. The reverse hydrogenation reaction was also accomplished, resulting in full hydrogenation of the generated oxalamides back to the corresponding amines and ethylene glycol, using the same catalyst. A plausible catalytic mechanism is proposed, supported by stoichiometric reactions, NMR studies, X-ray crystallography as well as the observation of some plausible intermediates. Further detailed mechanistic investigations and applications of this methodology are underway.

Conflicts of interest

There are no conflicts to declare

Acknowledgements

This research was supported by the European Research Council (ERC AdG 692775). D. M. holds the Israel Matz Professorial Chair of Organic Chemistry. Y.-Q. Z. acknowledges the Sustainability and Energy Research Initiative (SAERI) of Weizmann Institute of Science for a research fellowship.

Notes and references

1 J. T. Njardarson, Poster: *Top 200 Pharmaceutical Products by Retail Sales in 2018*.

2 (a) F. Curreli, S. Choudhury, I. Pyatkin, V. P. Zagorodnikov, A. K. Bulay, A. Altieri, Y. D. Kwon, P. D. Kwong and A. K. Debnath, *J. Med. Chem.*, 2012, **55**, 4764–4775; (b) F. Curreli, Y. D. Kwon, H. Zhang, Y. Yang, D. Scacalossi, P. D. Kwong and A. K. Debnath, *Antimicrob. Agents Chemother.*, 2014, **58**, 5478–5491.

3 (a) Z. Chen, Y. Jiang, L. Zhang, Y. Guo and D. Ma, *J. Am. Chem. Soc.*, 2019, **141**, 3541–3549; (b) W. Zhou, M. Fan, J. Yin, Y. Jiang and D. Ma, *J. Am. Chem. Soc.*, 2015, **137**, 11942–11945; (c) S. De, J. Yin and D. Ma, *Org. Lett.*, 2017, **19**, 4864–4867; (d) M. Fan, W. Zhou, Y. Jiang and D. Ma, *Org. Lett.*, 2015, **17**, 5934–5937; (e) G. G. Pawar, H. Wu, S. De and D. Ma, *Adv. Synth. Catal.*, 2017, **359**, 1631–1636; (f) V. S. Chan, S. W. Krabbe, C. Li, L. Sun, Y. Liu and A. J. Nett, *ChemCatChem*, 2019, **11**, 5748–5753; (g) D. V. Morarji and K. K. Gurjar, *Organometallics*, 2019, **38**, 2502–2511.

4 K. Abdelmajid and W. Cornelis, WO 2011095533 A1, 2011.

5 (a) J. G. Croissant, Y. Faticieiev, K. Julfakyan, J. Lu, A. Emwas, D. H. Anjum, H. Omar, F. Tamanoi, J. I. Zink and N. M. Khashab, *Chem.-Eur. J.*, 2016, **22**, 14806–14811; (b) Y. Faticieiev, J. G. Croissant, K. Julfakyan, L. Deng, D. H. Anjum, A. Gurinov and N. M. Khashab, *Nanoscale*, 2015, **7**, 15046–15050.

6 D. Ma, W. Zhou, M. Fan, H. Wu, J. Yin and S. Xia, US Pat. 20180207628 A1, 2018.

7 (a) R. Mancuso, D. S. Raut, N. D. Ca', F. Fini, C. Cargagna and B. Gabriele, *ChemSusChem*, 2015, **8**, 2204–2211; (b) K. Dong, S. Elangovan, R. Sang, A. Spannenberg, R. Jackstell, K. Junge, Y. Li and M. Beller, *Nat. Commun.*, 2016, **7**, 12075; (c) K. Şeker, D. Bariş, N. Arslan, Y. Turgut, N. Pirinçcioğlu and M. Toğrul, *Tetrahedron: Asymmetry*, 2014, **25**, 411–417; (d) B. P. Woods, M. Orlandi, C.-Y. Huang, M. S. Sigman and A. G. Doyle, *J. Am. Chem. Soc.*, 2017, **139**, 5688–5691.

8 C. Gunanathan, Y. Ben-David and D. Milstein, *Science*, 2007, **317**, 790–792.

9 (a) H. Zeng and Z. Guan, *J. Am. Chem. Soc.*, 2011, **133**, 1159–1161; (b) B. Gnanaprakasam, E. Balaraman, C. Gunanathan and D. Milstein, *J. Polym. Sci., Part A: Polym. Chem.*, 2012, **50**, 1755–1765.

10 (a) L. U. Nordstrøm, H. Vogt and R. Madsen, *J. Am. Chem. Soc.*, 2008, **130**, 17672–17673; (b) A. J. A. Watson, A. C. Maxwell and J. M. J. Williams, *Org. Lett.*, 2009, **11**, 2667–2670; (c) A. Prades, E. Peris and M. Albrecht, *Organometallics*, 2011, **30**, 1162–1167; (d) T. Zweifel, J.-V. Naubron and H. Grützmacher, *Angew. Chem., Int. Ed.*, 2009, **48**, 559–563; (e) S. C. Ghosh, S. Muthaiah, Y. Zhang, X. Xu and S. H. Hong, *Adv. Synth. Catal.*, 2009, **351**, 2643–2649; (f) D. Srimani, E. Balaraman, P. Hu, Y. Ben-David and D. Milstein, *Adv. Synth. Catal.*, 2013, **355**, 2525–2530.

11 (a) P. Hu, E. Fogler, Y. Diskin-Posner, M. A. Iron and D. Milstein, *Nat. Commun.*, 2015, **6**, 6859; (b) P. Hu, Y. Ben-David and D. Milstein, *Angew. Chem., Int. Ed.*, 2016, **55**, 1061–1064; (c) A. Kumar, T. Janes, N. A. Espinosa-Jalapa and D. Milstein, *J. Am. Chem. Soc.*, 2018, **140**, 7453–7457; (d) Y. Xie, P. Hu, Y. Ben-David and D. Milstein, *Angew. Chem., Int. Ed.*, 2019, **58**, 5105–5109; (e) J. Kothandaraman, S. Kar, R. Sen, A. Goeppert, G. Olah and G. K. S. Prakash, *J. Am. Chem. Soc.*, 2017, **139**, 2549–2552; (f) Z. Shao, Y. Li, C. Liu, W. Ai, S.-P. Luo and Q. Liu, *Nat. Commun.*, 2020, **11**, 591.

12 H. Yue, Y. Zhao, X. Ma and J. Gong, *Chem. Soc. Rev.*, 2012, **41**, 4218–4244.

13 A. Wang and T. Zhang, *Acc. Chem. Res.*, 2013, **46**, 1377–1386.

14 Y.-Q. Zou, N. von Wolff, A. Anaby, Y. Xie and D. Milstein, *Nat. Catal.*, 2019, **2**, 415–422.

15 J. Zhang, G. Leitus, Y. Ben-David and D. Milstein, *J. Am. Chem. Soc.*, 2005, **127**, 10840–10841.

16 D. Milstein, E. Balaraman, C. Gunanathan, B. Gnanaprakasam and J. Zhang, US Pat. 20130281664 A1, 2013.

17 E. Fogler, J. A. Garg, P. Hu, G. Leitus, L. J. W. Shimon and D. Milstein, *Chem.-Eur. J.*, 2014, **20**, 15727–15731.

18 (a) S. A. Lawrence, *Amines: Synthesis, Properties and Applications*, Cambridge University Press, Cambridge, 2004; (b) P. Roose, K. Eller, E. Henkes, R. Rossbacher and H. Höke, *Amines, Aliphatic*, in *Ullmann's Encyclopedia of Industrial Chemistry*, Wiley-VCH, Weinheim, 2015.

19 (a) E. Balaraman, B. Gnanaprakasam, L. J. W. Shimon and D. Milstein, *J. Am. Chem. Soc.*, 2010, **132**, 16756–16758; (b) M. Ito, T. Ootsuka, R. Watari, A. Shiibashi, A. Himizu and T. Ikariya, *J. Am. Chem. Soc.*, 2011, **133**, 4240–4242; (c) J. M. John and S. H. Bergens, *Angew. Chem., Int. Ed.*, 2011, **50**, 10377–10380; (d) J. R. Cabrero-Antonino, E. Alberico, H. J. Drexler, W. Baumann, K. Junge, H. Junge and M. Beller, *ACS Catal.*, 2016, **6**, 47–54; (e) N. M. Rezayee, D. C. Samblanet and M. S. Sanford, *ACS Catal.*, 2016, **6**, 6377–6383; (f) V. Papa, J. R. Cabrero-Antonino, E. Alberico, A. Spanneberg, K. Junge, H. Junge and M. Beller, *Chem. Sci.*, 2017, **8**, 3576–3585; (g) N. Gorgas and K. Kirchner, *Acc. Chem. Res.*, 2018, **51**, 1558–1569; (h) F. Kallmeier and R. Kempe, *Angew. Chem., Int. Ed.*, 2018, **57**, 46–60.

20 (a) H. Grützmacher, *Angew. Chem., Int. Ed.*, 2008, **47**, 1814–1818; (b) J. I. van der Vlugt and J. N. H. Reek, *Angew. Chem., Int. Ed.*, 2009, **48**, 8832–8846; (c) G. E. Dobereiner and R. H. Crabtree, *Chem. Rev.*, 2010, **110**, 681–703; (d) J. R. Khusnutdinova and D. Milstein, *Angew. Chem., Int. Ed.*, 2015, **54**, 12236–12273; (e) K. Sordakis, C. Tang, L. Vogt, H. Junge, P. J. Dyson and M. Beller, *Chem. Rev.*, 2018, **118**, 372–433.

21 O. Blum and D. Milstein, *J. Organomet. Chem.*, 2000, **593–594**, 479–484.

22 H. Li, X. Wang, F. Huang, G. Lu, J. Jiang and Z.-X. Wang, *Organometallics*, 2011, **30**, 5233–5247.

23 The reaction of glycolaldehyde dimer 1,4-dioxane-2,5-diol with **8a** also produced product **9a** in 62% isolated yield under optimal conditions, which further supports glycolaldehyde as a likely intermediate in this transformation.

